Applied Catalysis A, General 618 (2021) 118136

Contents lists available at ScienceDirect

Applied Catalysis A, General

journal homepage: www.elsevier.com/locate/apcata

Highly active solid oxide acid catalyst for the synthesis of benzaldehyde glycol acetal

Xiaoxiang Han [a,*], Jinwang Cai [a], Xiaorui Mao [a], Xinya Yang [a], Linyan Qiu [a], Fanghao Li [a], Xiujuan Tang [b], Yanbo Wang [a,*], Shang-Bin Liu [c]

[a] Department of Applied Chemistry, Zhejiang Gongshang University, Hangzhou, 310018, China
[b] College of Environmental Science and Engineering, Zhejiang Gongshang University, Hangzhou, 310018, China
[c] Institute of Atom and Molecular Sciences, Academia Sinica, Taipei, 10617, Taiwan

ARTICLE INFO

Keywords:
Composite metal oxide catalyst
Acetalization reaction
Process optimization
Response surface methodology

ABSTRACT

A series of composite metal oxide catalysts, namely CeMnTiO, CeCoTiO, and CeFeTiO, were prepared by sol-gel method, and their physicochemical properties were characterized by various techniques, *viz*. SEM, XRD, XPS, and NH_3-TPD. Their desirable acidity and surface area were suitable for the acid-catalyzed acetalization reaction of benzaldehyde (BzH) with ethylene glycol (EG). In particular, CeFeTiO catalyst exhibited superior activity and excellent durability, leading to an acetal yield of 96.8 %, which was in close agreement with the optimal yield (96.95 %) predicted by the response surface methodology (RSM) based on a Box-Behnken design (BBD). Moreover, a kinetic study under the optimal reaction conditions showed that the acetalization reaction was second-order with an active energy (E_a) of 46.65 kJ/mol. Results revealed that CeFeTiO catalyst had high efficiency to surpass conventional Amberlyst catalysts for acetalization reactions.

1. Introduction

Acetals, produced from aldehydes or ketones, were normally used as protective groups for carbonyl groups in organic synthesis owing to their stability and low reactivity in basic media [1–4]. This feature expanded acetals' applications to food and beverage industries [4–10]. Acetalization, a process to generate acetals, was an acid-catalyzed reaction over various protonic and aprotic catalysts such as H_2SO_4, HCl, H_3PO_4, heteropolyacids, niobic acid ($Nb_2O_5{\cdot}nH_2O$), zeolites, molecular sieves, and ionic liquids *etc*. However, these traditional acid catalysts possessed various disadvantages such as corrosiveness, hazardous to the environment, cost in waste management, tedious in operation and product separation, and so on [11–15]. The perspectives of industrial production and environmental protection encouraged solid acid catalyst innovation to achieve environmental benign and high efficiency. In this context, metal oxides had drawn considerable attention as solid acid catalysts. For example, Ti^{4+}-exchanged montmorillonite was utilized for acetalization of various carbonyl compounds, nonetheless, its catalytic performance was still limited due to its poor thermal stability, low surface area, weak water tolerance ability, inferior pore size, and so on [16–25].

Recently, catalysts based on assorted composite metal oxides were developed and were applied in various reactions. For example, niobium-aluminum-based catalysts synthesized by a sol-gel process were successfully applied in acetalization of acetone [26]. These Nb/Al-based mixed oxides showed excellent catalytic activity with the conversion rate of glycerol up to 84 %. And Olutoye and co-workers utilized eggshell, which was treated by magnesium nitrate and potassium nitrate, as a catalyst for transesterification of palm oil to produce fatty acid methyl esters(FAME) with high yield (85.8 %) [27], much better than the performance of conventional counterparts, such as $K_2Mg_{0.34}Zn_{1.66}O_3$, in the same chemical reaction with 73 % yield [28]. Moreover, the presence of surface promoters such as La_2O_3 and ZrO_2 enhanced the catalytic activity of mixed metal oxides such as CuO/MgO [29]. This was ascribed to the doping process to boost the amount of catalytically active sites on the surface of the catalyst. All endowed composite metal oxides not only to overcome the shortcomings of single metal oxides but also to furnish beneficial characteristics such as desirable surface area and pore structure, as well as high hydrothermal stability.

We reported herein, the synthesis of a series of composite metal oxide catalysts, CeMnTiO, CeCoTiO, CeFeTiO, CeTiO, and FeTiO, by means of a sol-gel method. The catalytic performances of these

* Corresponding authors.
E-mail addresses: hxx74@126.com (X. Han), wangyb7822@126.com (Y. Wang).

https://doi.org/10.1016/j.apcata.2021.118136
Received 30 September 2020; Received in revised form 31 March 2021; Accepted 1 April 2021
Available online 7 April 2021

composite catalysts in acetalization of benzaldehyde (BzH) and ethylene glycol (EG) were assessed. In parallel, their physicochemical properties were characterized by a variety of techniques such as SEM, FT-IR, XRD, XPS, physisorption, and NH_3-TPD. Results displayed that CeFeTiO had various advantages such as desirable acidity, appropriate surface area, superior catalytic activity and recyclability for acetal production, and overcame the shortcomings of traditional acid catalysts and single metal oxide. Moreover, the response surface methodology (RSM) was applied to optimize this process. Its kinetics was probed as well. All studies offered insights for efficient production of acetal.

2. Experimental

2.1. Materials and catalyst preparation

n-butyl titanate ($C_{16}H_{36}O_4Ti$), iron nitrate ($Fe(NO_3)_3{\cdot}9H_2O$), cobalt nitrate ($Co(NO_3)_2{\cdot}6H_2O$), cerium nitrate ($Ce(NO_3)_3{\cdot}6H_2O$), silver nitrate ($AgNO_3$), neodymium nitrate ($Nd(NO_3)_3{\cdot}6H_2O$), praseodymium nitrate ($Pr(NO_3)_3{\cdot}6H_2O$), nickel nitrate ($Ni(NO_3)_2{\cdot}6H_2O$), cupric chloride ($CuCl_2$), stannous chloride ($SnCl_2$), zinc chloride ($ZnCl_2$), chromium trichloride ($CrCl_3$), manganese chloride ($MnCl_2$), anhydrous ethanol (C_2H_5OH), hydrochloric acid (HCl), benzaldehyde (BzH; C_6H_5CHO), ethylene glycol (EG; $(CH_2OH)_2$), and cyclohexane (C_6H_{12}) were obtained as analytical grade from commercial suppliers, and used without further purification unless otherwise specified.

2.2. Catalyst preparation

All composite metal oxides catalysts were synthesized by a sol-gel method. The preparation procedure of the CeFeTiO catalyst was picked up as an example. Known amounts of cerium nitrate and iron nitrate were dissolved together in distilled water at room temperature with desirable amounts of ethanol and *n*-butyl titanate. Subsequently, a small amount (2 mL) of hydrochloric acid was added into the mixture solution under stirring condition to form a sol. Finally, the obtained gel was aged for 24 h at room temperature before it was calcined at 300 °C in static air for 5 h. Metal nitrate or chloride was used as raw material. A similar procedure was employed for the preparation of other composite metal oxides catalysts.

2.3. Catalyst characterization

The physicochemical properties of various catalysts were characterized by a variety of techniques. X-ray diffraction (XRD) analyses were conducted on a Rigaku Ultimate IV equipped with a Cu Kα source operating at 40 kV and 20 mA. Each XRD profile was recorded by a scanning rate of 0.02°/minute over a range of 2θ angle of 5–80°. N_2 adsorption/desorption isotherm measurements were performed on a Quantachrome Autosorb-1 apparatus at 77 K. The total surface area of catalyst sample was derived bythe Brunauer-Emmett-Teller (BET) method. Temperature-programmed desorption of ammonia (NH_3-TPD) was utilized to characterize the acidity of catalyst. Prior to the adsorption of NH_3, each catalyst sample was first subjected to heat pretreatment in flowing He gas environment at 400 °C for 60 min, then slowly cooled to 80 °C before the measurement. Each sample was treated in a mixture of 2% NH_3-98 % He (V/V) at 80 °C for 60 min. Then, the adsorbate-loaded sample was heated from 80 to 900 °C at a rate of 10 °C/min under flow of He. The amount of desorbed NH_3 was monitored by a thermal conductivity detector (TCD) after the effluent gas was filtered by a water trap with pelletized sodium hydroxide. X-ray photoelectron spectroscopy (XPS) was used to probe the surface properties of catalyst. The XPS determination was performed on a VG Scientific ESCALab220i-XL spectrometer equipped with a typical laboratory-scale Al Kα source and an operation power of 300 W. A Hitachi SU8010 scanning electron microscope (SEM) was used to investigate the morphology of catalyst. An Oxford X-Maxenergy dispersive spectrometer (EDS) was used for analyzing the compositions of chemical elements. A Mettler Toledo thermogravimetric Analysis (TGA) was used to examine the thermal stabilities of various catalysts.

2.4. Catalytic reaction

The catalytic performance of composite metal oxide catalysts were assessed by the acetalization of benzaldehyde (BzH) with ethylene glycol (EG). The acetalization reaction was carried out in a 100 ml three-necked flask equipped with a water separator, a stir bar, and a reflux condenser. In brief, the reaction mixture consisting of BzH (10.6 g, 0.1 mol), EG (9.9 g, 0.16 mol), a catalyst (0.6 g), and the water carrying agent (*i.e.*, cyclohexane, 12 mL) was heated under stirring (450 rpm) and reflux conditions for a desirable period of time in an oil bath. Upon completion, the mixture was cooled to room temperature, followed by the separation of the catalyst. For recycling tests, the spent catalyst was washed with ethyl acetate, dried under vacuum at 70 °C for 10 h before reuse. The product of the corresponding reaction was quantitatively analyzed by a gas chromatography (Agilent 7890B) equipped with a flame ionization detection (FID) and an HP-5 capillary column. Compared with the authentic sample, biphenyl as the internal standard, reactants and products were identified. The yield of acetal, colorless and transparent liquid with fruity aroma, was collected by the atmospheric distillation at the specific temperature range of 224–228 °C.

2.5. Experimental design and mathematical model

The response surface methodology (RSM) was employed to optimize the synthesis process of benzaldehyde glycol acetal (BEGA) with CeFeTiO as a catalyst. The Box-Behnken design (BBD) experiment was employed to evaluate the correlations between the acetal yield and the control process variables, namely the molar ratio of glycol/benzaldehyde (x_1), the reaction time (x_2), the amount of catalyst (x_3), and the amount of water-carrying agent (x_4).

According to the 3^4 full-factorial central composite designs and the principle of BBD, these four aforementioned control process variables were tested by means of three levels, namely −1, 0, and +1, as depicted in Table 1. Accordingly, an experimental design containing 29 points was adopted, including 24 factor points and 5 center points, as depicted in Table 2. The response of the experimental design, denoted *Y*, was expressed as

$$Y = \beta_0 + \sum_{i=1}^{k} \beta_i x_i + \sum_{i=1}^{k} \beta_{ii} x_i^2 + \sum_{j=1}^{k} \beta_{ij} x_i x_{ij} + \varepsilon \quad (1)$$

where *Y* was the predicted response; x_i and x_j (i & $j = 1$–k) were the coded levels of various independent variables; while β_0, β_i, β_{ii}, and β_{ij} denoted the regression coefficients representing the offset term, main, quadratic, and interaction effect, respectively; *k* represented the total number of design variables; ε was the random error.

2.6. Kinetic study

The rate equation for acetalization reaction of BzH and EG over the CeFeTiO catalyst may be defined as:

Table 1
List of symbols for different process variables and corresponding coded levels and ranges used in the experimental design.

Variable (unit)	Symbol	Range and level		
		−1	0	+1
EG/BzH ratio (mol/mol)	x_1	1.5	1.6	1.7
Reaction time (h)	x_2	2.5	3	3.5
Amount of catalyst (wt%)	x_3	5	6	7
Amount of cyclohexane (mL)	x_4	10	12	14

Table 2
List of experimental designs and corresponding response values obtained for acetalization reaction over the CeFeTiO catalyst.

Run	Variable and level				BEGA yield (%)	
	x_1	x_2	x_3	x_4	Experimental	Calculated
1	−1	−1	0	0	82.54	82.63
2	1	−1	0	0	86.36	86.68
3	−1	1	0	0	88.03	88.61
4	1	1	0	0	83.70	84.50
5	0	0	−1	−1	87.05	88.52
6	0	0	1	−1	85.50	85.34
7	0	0	−1	1	82.10	83.16
8	0	0	1	1	95.80	95.23
9	−1	0	0	−1	90.84	90.82
10	1	0	0	−1	86.58	86.53
11	−1	0	0	1	88.93	88.83
12	1	0	0	1	93.19	93.06
13	0	−1	−1	0	83.57	83.20
14	0	1	−1	0	80.38	80.07
15	0	−1	1	0	82.45	82.61
16	0	1	1	0	89.32	89.54
17	−1	0	−1	0	87.94	87.11
18	1	0	−1	0	85.00	83.98
19	−1	0	1	0	88.19	88.46
20	1	0	1	0	91.44	91.52
21	0	−1	0	−1	81.20	80.85
22	0	1	0	−1	89.57	88.67
23	0	−1	0	1	88.89	89.04
24	0	1	0	1	85.42	85.02
25	0	0	0	0	94.20	93.60
26	0	0	0	0	93.93	93.60
27	0	0	0	0	93.00	93.60
28	0	0	0	0	93.27	93.60
29	0	0	0	0	93.60	93.60

$$r = -\frac{dC_A}{dt} = k_+ C_A^{\alpha} C_B^{\beta} - k_- C_C^{\gamma} C_D^{\eta} \quad (2)$$

where r represented the reaction rate based on benzaldehyde consumption; k_+ and k_- stood for the forward and reverse rate constants, respectively; C_A, C_B, C_C, and C_D denoted the concentrations of BzH, EG, acetal, and water, respectively; and α, β, γ and η were their partial orders.

In view of the fact that water was effectively and continuously removed by the water-carrying agent, cyclohexane, throughout the acetalization reaction, the reaction was considered as an irreversible process to ignore the second term in Eq. (2) with a simple expression.

$$r = -\frac{dC_A}{dt} = kC_A^{\alpha} C_B^{\beta} \quad (3)$$

For the sake of simplification, it was assumed that $\alpha = \beta = 1$. In addition, $Q = C_{B0} - C_{A0}$, whereas C_{A0} and C_{B0} denoted initial concentration of BzH and EG (both in unit of mol/L). Then, $C_B = C_A + Q$, and Eq. (3) may be rewritten as:

$$r = -\frac{dC_A}{dt} = kC_A(C_A + Q) \quad (4)$$

Taking the natural logarithm on both sides of the equation, Eq. (4) may further be expressed as:

$$\ln\frac{CA + Q}{CA} = Qkt + C \text{ or} \ln\frac{CA}{CB} = (CAO - CBO)kt + C \quad (5)$$

With the aid of the Origin 8.0 program, the values of k and C were assessed via the linear fitting operation of $\ln C_A/C_B$ via t under different temperatures. The Arrhenius equation,

$$\ln k = \ln k_0 - \frac{E_a}{R}\frac{1}{T} \quad (6)$$

was utilized to estimate the pre-exponential factor (k_0) and the activation energy (E_a).

3. Results and discussion

3.1. Catalyst characterization

The SEM and EDX profiles of the CeFeTiO catalyst were illustrated in Fig. 1. The catalyst clearly showed rough surface deposited with irregular particles. Further analysis of the EDS spectrum (Fig. 1b) revealed that the CeFeTiO catalyst was indeed constituted by primary elements such as Ti, Ce, Fe, and O, as expected. As it will be shown later (*vide infra*) that mutual bonding interaction among these elements led to formation of porosity. This, together with the predominant presence of active Ti metal centers were crucial factors for the improved catalytic activity observed [30,31]. Table 3 revealed the results for elemental analysis of CeFeTiO catalyst. It was observed that strong presence of Ti in weight percentage indicated highly acidity of the prepared catalyst.

Fig. 2 showed the XRD patterns of the CeFeTiO catalyst calcined at different temperatures. For sample calcined at a lower calcination temperature (200 °C), diffraction peaks with characteristics of anatase TiO_2 (JCPDS card no. 21-1272), CeO_2 (JCPDS card no. 34-0394.), α-Fe_2O_3 (JCPDS card no. 39-1346), and $Fe_3Ti_3O_{10}$ (JCPDS card no. 43-1011) were observed. Upon increasing the calcination temperature, the primary diffraction peak of 2θ at *ca.*25.4° shifted toward lower value mainly due to the removal of CO_2, HCl, and H_2O, indicating the mixture formation of Fe and Ti atoms in the CeFeTiO sample during the calcination process [30]. This observation was consistent with the results of EDX analysis. Moreover, the intensities of diffraction peaks responsible for CeO_2, α-Fe_2O_3, and TiO_2 were found to increase with increasing calcination temperature, indicating the sintering and agglomeration of these single metal oxides, which were unfavorable for acetalization reaction. These phenomena were readily observed for the sample calcined at 400 °C. By comparison, the CeFeTiO catalyst calcined at 300 °C, which was found to exhibit the highest catalytic activity (*vide infra*), exhibited a well-distributed metal oxide species associated with various constituent elements such as Fe, Ti, Ce, and O.

In Fig. 3, the surface properties of the fresh and spent CeFeTiO catalysts were investigated. The XPS spectrum obtained at various core levels for the spent CeFeTiO were nearly identical to that of its fresh counterpart, except for those at Ce 3d and Ti 2p core levels near 905 and 472.5 eV, respectively. The Ce 3d XPS spectrum (Fig. 3a) revealed the presences of Ce^{4+} characteristic peaks at 898.57 and 882.25 eV, indicating the presence of CeO_2 in the CeFeTiO catalyst. Moreover, the spectrum observed for the Fe 2p core level (Fig. 3b) exhibited two Fe^{3+} characteristic peaks at 724.60 and 711.04 eV, revealing the presence of Fe_2O_3. The Ti 2p XPS spectrum showed two main peaks at 464.28 and 458.56 eV (Fig. 3c), which may be attributed to the presence of Ti^{3+} in CeFeTiO. In addition, the presence of the O^{2-} characteristic peak at 529.99 eV in the O 1s XPS spectrum in Fig. 3d certified that oxygen atom was indeed connected to Ce, Fe, and Ti metal ions in divalent forms, in excellent agreement with the XRD results of CeO_2, α-Fe_2O_3, and TiO_2 presence in Fig. 2. Both the fresh and spent catalysts exhibited similar XPS spectrum, which hinted that the oxidation states of primary metal species in the CeFeTiO catalyst were independent of their participation in the acetalization reaction.

Since the specific surface area and the total pore volume of the catalyst affect its catalytic performances, they were assessed by BET analyses based on N_2 adsorption- desorption isotherm measurements (not shown). In Table 4, the BET surface areas (S_{BET}) of FeTiO and CeTiO samples were 55.9 and 72.1 m^2/g, respectively, which were dramatically lower than that of the CeFeTiO catalyst (94.4 m^2/g). Likewise, CeFeTiO samples had higher total pore volume (V_{Tot}) (0.19 cm^3/g) than both FeTiO (0.13 cm^3/g) and CeTiO (0.14 cm^3/g) samples. All inferred that the introduction of a third metal promoter notably enhanced textural properties of the composite metal oxide catalyst. It was anticipated that a higher pore volume possessed by the catalyst rendered access of a greater amount of reactants within the catalyst, which in turns was favorable for acetal formation. The above notion was in line

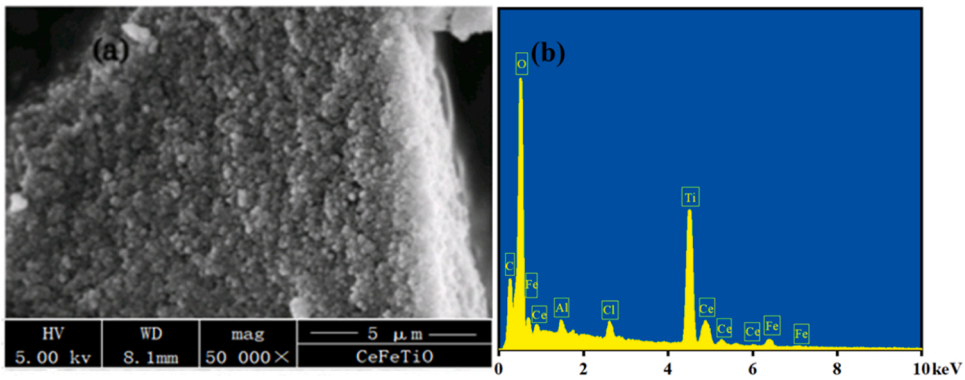

Fig. 1. (a) a SEM image and (b) a EDS profile of the CeFeTiO catalyst.

Table 3
Elemental analysis (EDS) of as-synthesized CeFeTiO catalyst.

Elements	CeFeTiO	
	Atom(%)	Weight(%)
Titanium (Ti)	17.11	32.60
Oxygen (O)	78.74	50.12
Iron (Fe)	1.74	3.86
Cerium (Ce)	2.41	13.42
Total	100	100

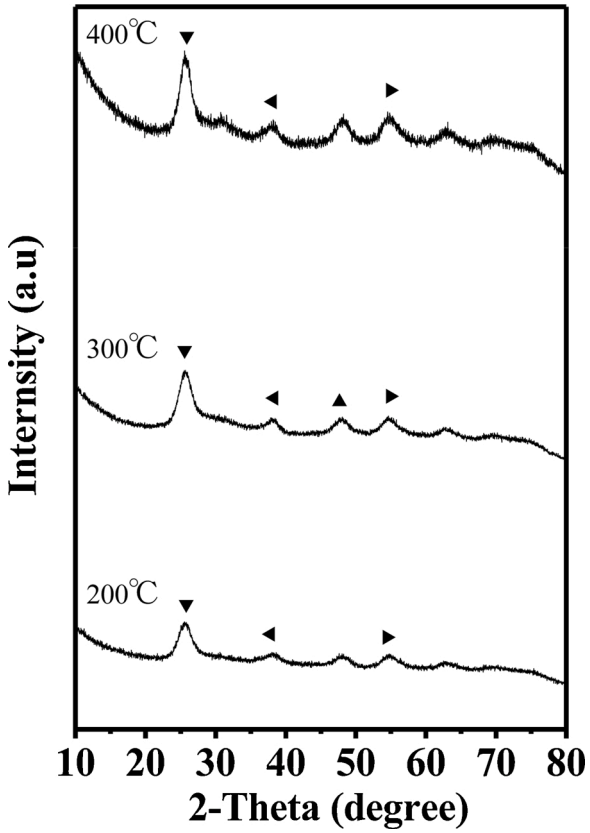

Fig. 2. Powder XRD patterns of the CeFeTiO catalyst calcined at different temperatures for 5 h. Symbols notations: ▼: α-Fe_2O_3, $Fe_3Ti_3O_{10}$, CeO_2;◀: TiO_2, α-Fe_2O_3; ▲: α-Fe_2O_3, CeO_2; ▶: α-Fe_2O_3, CeO_2;●:α-Fe_2O_3; ◆: TiO_2, α-Fe_2O_3, CeO_2.

with the observed catalytic results, a superior activity of the CeFeTiO catalyst compared to FeTiO and CeTiO (*vide infra*).

The acid properties of various catalysts were also characterized by the temperature program desorption of ammonia (NH_3-TPD) with two parameters, the temperature of desorption peak emergence to reflect the catalyst acidic strength and the peak's integrated area to assess acid concentrations in TCD profiles [32–34]. Since strong acid sites should be associated with a higher binding energy with ammonia, hence resulted in desorption peaks at higher temperatures. As such, desorption peak appear at low temperatures (< 250 °C) may be referred as acid sites with weak acidity, whereas acid sites with medium acidic strengths should show desorption peaks centering in the temperature range between (250–450 °C). Likewise, desorption peaks emerging at high temperatures (≥450 °C) represented the presences of strong acid sites [34]. In particular, sites with desorption peaks at elevated temperatures (> 700 °C) were ultra-strong acidic. The FeTiO catalyst with four desorption peaks at 290, 498, 700, and 765 °C respectively (Fig. 4b), clearly indicated the predominant existence of ultra-strong acid sites. Whereas, the CeTiO catalyst possessing two desorption peaks at 195 and 800 °C with comparable peak areas (Fig. 4c) hinted the presences of weak and ultra-strong acid sites. On the other hand, the TCD profile of the CeFeTiO catalyst exhibited three desorption peaks at 245, 450, and 697 °C (Fig. 4a), which implied the existence of three types of sites with weak, medium, and strong acidity, respectively. In addition, the peak centering at 245 °C with much greater integrated area than that of higher temperature peaks suggested that the CeFeTiO catalyst possessed mostly acid sites with weaker acidity. Desirable weak and medium acidity of CeFeTiO catalyst was responsible for high catalytic activity (*vide infra*). Similar arguments were obtained based on TCD profiles of CeFeTiO, CeCoTiO, and CeMnTiO catalysts (Fig. 4d–4f). It was noteworthy that both catalysts, CeCoTiO and CeMnTiO, possessed more sites with ultra-strong acidities, revealed by the predominant peaks at elevated temperatures (T > 700 °C).

3.2. Catalyst activity

The catalytic performances of various composite metal oxide catalysts in acetalization of benzaldehyde with ethylene glycol were depicted in Table 4. For the acetal yield, its experiment error of less than 1% was inferred by data obtained from both GC analyses and distillation operations. FeTiO and CeTiO (Entries 1 and 2: Table 4), which possessed less acidic sites with relatively weak acidities showed inferior catalytic activity for acetalization of benzaldehyde, leading to an acetal yield of 68.8 % and 70.7 %, respectively. The introduction of a third component onto the above FeTiO and CeTiO (Entries 3–14; Table 4) significant improved their catalytic activities, which partially came from their acidity enhancement (cf. Fig. 4f vs d). The only exception was CeCoTiO catalyst (Entry 8) with an inferior acetal yield of 56.7 % and was blamed to much lower S_{BET} (36.0 m^2/g) and V_{Tot} (0.10 cm^3/g) as well as weaker

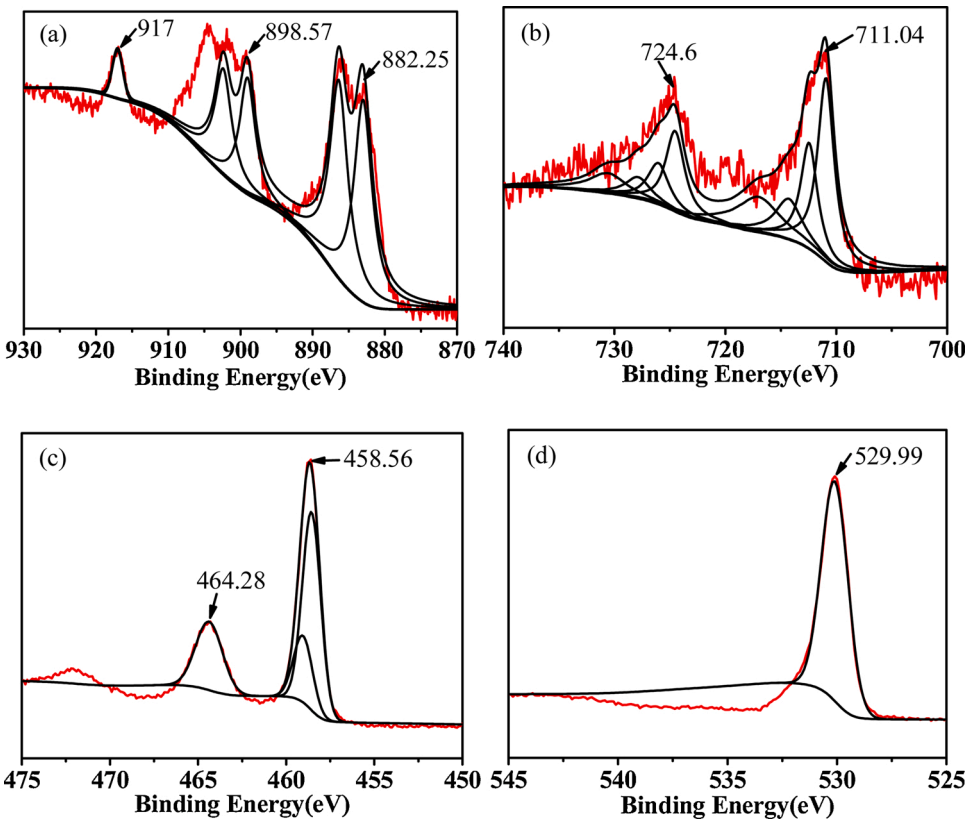

Fig. 3. XPS spectra of the (a) Ce3d (b) Fe2p (c) Ti2p, and (d) O1 score levels observed for the fresh (black curve) and spent(red curve) CeFeTiO catalysts.

Table 4
Catalytic performances and surface area of various catalysts during acetalization of benzaldehyde with ethylene glycol[a].

Entry	Catalyst	S_{BET} (m^2/g)[b]	V_{Tot} (cm^3/g)[b]	BEGA yield(%)	
				EA[c]	Distillation[d]
1	FeTiO	55.9	0.13	69.4	68.8
2	CeTiO	72.1	0.14	71.2	70.7
3	FeNdTiO	88.4	0.16	86.4	85.7
4	FePrTiO	84.3	0.15	83.8	83.1
5	FeSnTiO	90.9	0.17	88.3	87.6
6	CeFeTiO	94.4	0.19	94.2	93.6
7	CeMnTiO	47.0	0.12	79.1	78.5
8	CeCoTiO	36.0	0.10	57.1	56.7
9	CeNiTiO	86.2	0.16	84.4	83.6
10	CeCuTiO	85.4	0.15	84.9	84.2
11	CeAgTiO	34.6	0.09	84.5	83.8
12	CeZnTiO	44.2	0.11	86.8	86.0
13	CeCrTiO	90.4	0.16	85.2	84.5
14	CeSnTiO	90.4	0.16	88.6	87.8

[a] Reactions conditions: glycol/benzaldehyde = 1.6 mol/mol; amount of catalyst = 6 wt%; reaction time = 3 h; amount of cyclohexane (water-carrying agent) = 12 mL; temperature =110 °C.
[b] Obtained from BET analysis based on N_2 adsorption-desorption isotherm data.
[c] Elemental analysis by GC.
[d] Analyzed by distillation.

acidity (cf. Fig. 4e vs d) compared to the other catalysts. Nonetheless, it was intriguing that the CeAgTiO catalyst (Entry 11), which possesses even lower S_{BET} (34.6 m^2/g) and V_{Tot} (0.09 cm^3/g) compared to its trimetal oxide counterparts exhibited a satisfactory acetal yield (83.8 %). This was most likely due to the enhancement in catalyst acidity upon introducing the Ag promotor. Among all composite catalysts in this study, the CeFeTiO catalyst (Entry 6) possessed the highest surface area (S_{BET} = 94.4m^2/g), the largest total pore volume (V_{Tot} = 0.19cm^3/g) and desirable acidity (Fig. 4c), and resulted in the best catalytic activity with a superior BEGA yield of 93.6 %. On the basis of the NH_3-TPD results in Fig. 4, the introduction of the third metal promotor onto FeTiO and CeTiO, the population of sites with both weak and medium acidic strengths increased, which indicated that the presence of acid sites with strong or ultra-strong acidic strengths was non-requisite or even detrimental in the acetalization reaction. On the other hand, textural properties such as specific surface area (S_{BET}) and pore volume (V_{Tot}) of the composite metal oxide catalysts appeared to be more important for catalytic performances during acetalization of BzH with EG. In summary, the catalytic activity observed for these trimetal oxide catalysts during acetalization reaction was mainly dictated by their textural properties (*i.e.*, specific surface area and pore volume) and concentrations of acid sites. Moreover, catalysts possessing acid sites with weak and medium acidic strengths seemed to be more favorable for the acetalization reaction than those with sites having strong or ultra-strong acidic strengths. Table 5 showed the acetalization over various catalyst reported by literature. Compare with these results, CeFeTiO catalyst showed excellent catalytic performance under mild reaction condition. The CeFeTiO catalyst had the advantages of good catalytic activity, simple preparation process and easy separation, so we choosed it as the catalyst for acetalization.

3.3. Effect of reaction parameters

The effects of experimental variables such as amounts of reactants (in terms EG/BzH molar ratio), catalyst, and water carrying agent (*i.e.*, cyclohexane) and reaction time on catalytic performances during acetalization of BzH with EG over the CeFeTiO catalyst were investigated. All experiments were carried out at 110 °C by varying one of the reaction variable while keeping the rest constant: EG/BzH = 1.6 mol/mol; amount of catalyst = 6 wt%; reaction time = 3 h; amount of cyclohexane = 12 mL, and the results were displayed in Fig. 5. As shown in

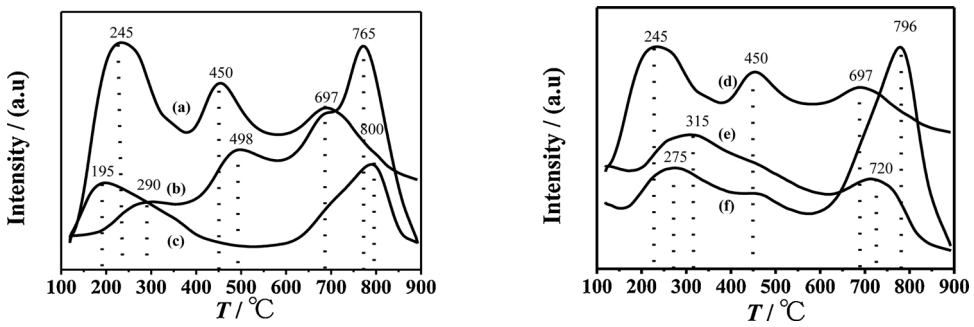

Fig. 4. NH_3-TPD revealing TCD signal intensity against temperature for various catalyst samples, left: (a) CeFeTiO, (b) FeTiO, (c) CeTiO, and right: (d) CeFeTiO, (e) CeCoTiO, and (f) CeMnTiO catalysts.

Table 5
Catalytic performances of various catalysts during acetalization.

Catalyst	Substrate	Catal. Am. (wt%)	Time (h)	Temp. (℃)	Yield (%)	Ref.
$Cs_{2.5}H_{0.5}PW_{12}O_{40}$	Formaldehyde + glycerol	26.6	1	70	70	[5]
$Cu_3(BTC)_2$	Benzaldehyde + methanol	3	24	25	88	[25]
Amberlyst 47	*n*-Butyraldehyde + glycerol	0.5	8	80	94	[35]
Nb15-HUSY	Acetone + glycerol	2	3	70	57	[6]
Hf-TUD-1	Acetone + glycerol	3	6	80	52	[19]
UiO-2−650	Benzaldehyde + methanol	–	6	–	86	[36]
Me-SBA15-Ar-SO_3H	Acetone + glycerol	5	0.5	70	80	[37]
Ni[MIMPSH]$PW_{12}O_{40}$	Benzaldehyde + glycol	5	3	110	94.6	[38]
CeFeTiO	Benzaldehyde + glycol	6.9	2.9	110	96.8	

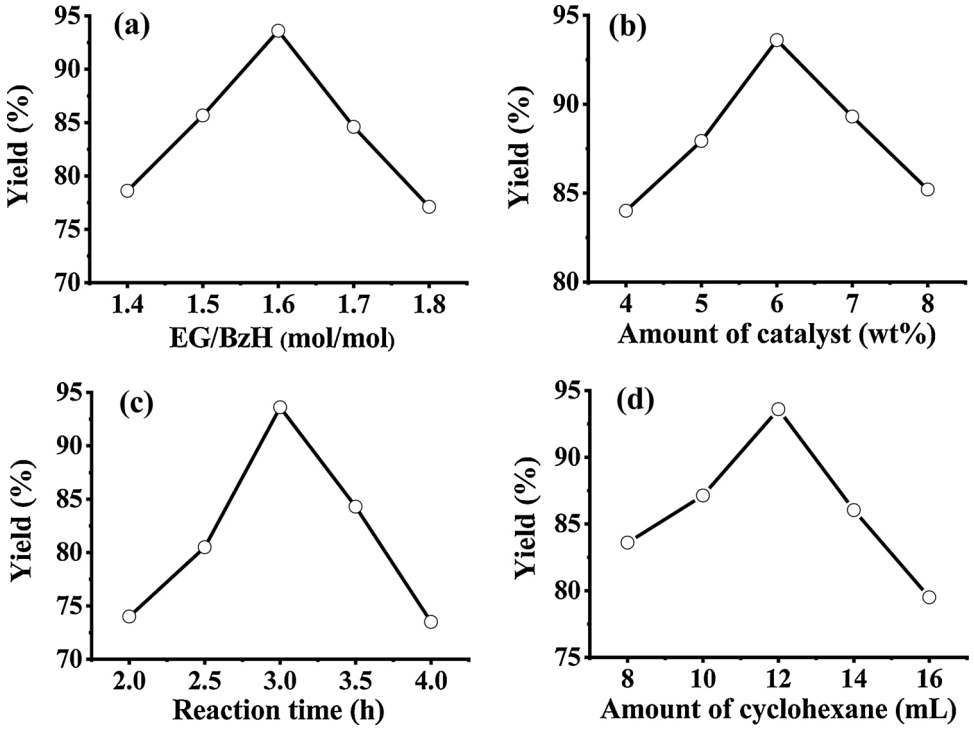

Fig. 5. Variations of BEGAyield over theCeFeTiO catalyst with (a) ethylene glycol/benzaldehydemolar ratio, (b) amount of catalyst, (c) reaction time, and (d) amount of watercarrying agent,cyclohexane.

Fig. 5a, the BEGA yield first increased with increasing amount of glycol, till reaching a peak value (93.6 %) at EG/BzH = 1.6 due to the fact that the reaction equilibrium was shifting towards acetal production. However, further increasing the amount of glycol tended to dilute the concentrations of benzaldehyde and the CeFeTiO catalyst, thus, resulted in a gradual decrease in acetal yield [38].

Similar dependences of acetal yield with catalyst amount, reaction time, and amount of cyclohexane were also observed, which all led to a maximum yield of 93.6 % at a catalyst amount of 6 wt% (Fig. 5b), a reaction time of 3 h (Fig. 5c), and a cyclohexane amount of 12 ml (Fig. 5d), respectively. It was clear that the number of available acid sites was dictated by the amount of catalyst, by which, when in excess would lead to promote undesirable side reactions to diminish the product selectivity, hence, decreased the acetal yield. Moreover, since

acetalization was a reversible reaction, while acetalization reaction toward formation of acetal was more favorable during initial reaction period, a prolonged reaction time may lead to formations of side products such as hemiacetals to spoil the acetal yield. In addition, since the continuous removal of water was crucial for sustaining the catalytic activity during the acetalization reaction. In this regard, cyclohexane was exploited as the water-carrying agent. However, the presence of an excessive amount of cyclohexane induced the dilution of reactant catalyst (acid sites), which in turn resulted in a decrease in the acetal yield.

3.4. Optimization of reaction parameters

The effects of reaction parameters on product yield were investigated by means of RSM based on an experimental Box-Behnken design(BBD). In this context, four independent experimental variables, namely the EG/BzH molar ratio (x_1), the reaction time (x_2), the amount of catalyst (x_3), and the amount of cyclohexane as the water-carrying agent (x_4) were chosen with three coded levels of experimental design and designated range (see Table 1). Accordingly, a 3^4 full-factorial experimental BBD with coded levels were exploited, leading to a total of 29 experimental sets, including 24 factorial points and 5 centering points (Table 2). Moreover, a second-order polynomial model equation given by RSM was used to reveal the interactive effects between experimental variables, to optimize the reaction process, as well as to predict the response (Y) of the experimental design. The yield of benzaldehyde ethylene glycol acetal (BEGA) was expressed by a quadratic equation:

$$Y = +93.60 - 0.017x_1 + 0.95x_2 + 2.22x_3 + 1.13x_4 - 2.04x_1^2 - 5.95x_2^2 - 3.79x_3^2 - 1.75x_4^2 - 2.04x_1x_2 + 1.55x_1x_3 + 2.13x_1x_4 + 2.51x_2x_3 - 2.96x_2x_4 + 3.81x_3x_4. \quad (7)$$

Accordingly, the fitted polynomial equation was further expressed by means of the response surface and the contour plots (*vide infra*) to visualize correlations between the response and experimental variables at different coded levels and to infer optimized process conditions. Moreover, analysis of variance (ANOVA) was applied to verify the fitting quality of the aforementioned quadratic model, and the results were summarized in Table 6. The significance of the model was assessed by comparing the F-value with its tabulated counterpart. In Table 6, the F-value of the model was 59.28, much greater than the tabulated F-value, which certified this model adequate and significant. In addition, p-value less than 0.0001 indicated the probability of such large "F-Value" close to the noise level. Compared to the pure error, the Lack of fit F-value of 3.4 was insignificant. In addition, the value of the coefficient of determination (R^2) 0.9834 revealed that this model was reliable and consistent to the experimental results. The "Adeq Precision" (26.43), defined by the ration of signal to noise, was also greater than the desirable value (4.0). The value of the coefficient of variation (CV) 0.91 % demonstrated that all experiments were reliably and reproducibly conducted with adequate signal-to-noise ratio. In summary, the aforementioned ANOVA results clearly indicated that the proposed model was highly reliable and the experimental design was also highly reasonable for the prediction of acetal yield over the CeFeTiO catalyst.

The corresponding contour plots as well as the three-dimensional (3D) response surface plots obtained from the predicted model were displayed in Figs. 6 and 7, respectively. In general, the interaction between a pair of reaction variables was inferred from the shape of contour plots. The presence of an elliptical or saddle shape of contour plot would indicate that the corresponding interaction was significant. On the other hand, contour plots with the nearly circular shape would reflect the weak or insignificant interaction between the variables. Moreover, the density of the response surface contour also reflected the influence of corresponding pair of variables on the response value. A denser contour curves would indicate a greater impact on the response value. Thus, the correlations between the reaction time (x_2) and the amount of catalyst (x_3) on acetal yield was highly significant (Figs. 7d and 8d). This was in excellent agreement with P-value (<0.0001) of x_2x_3 by ANOVA. By the same token, the same conclusions may also be drawn for x_1x_2, x_1x_4, x_2x_4, and x_3x_4. On the other hand, a weaker correlation between the EG/BzH ratio (x_1) and the amount of catalyst (x_3) was inferred from Figs. 7b and 8b, and was verified by ANOVA data (Table 6).

Table 6
Regression coefficients and corresponding F- and P-values obtained for the response of acetal yield based on ANOVA.

Source	Sum of square	DF[a]	Mean square	F	$P > F$	Significance[b]
Model	527.77	14	37.7	59.28	< 0.0001	**
x_1	3.333E-003	1	3.333E-003	5.242E-003	0.9433	
x_2	10.85	1	10.85	17.06	0.001	*
x_3	59.23	1	59.23	93.14	< 0.0001	**
x_4	15.39	1	15.39	24.2	0.0002	*
x_1^2	27.01	1	27.01	42.47	< 0.0001	**
x_2^2	229.96	1	229.96	361.62	< 0.0001	**
x_3^2	93.19	1	93.19	146.55	< 0.0001	**
x_4^2	19.85	1	19.85	31.21	< 0.0001	**
$x_1\,x_2$	16.61	1	16.61	26.11	0.0002	*
$x_1\,x_3$	9.58	1	9.58	15.06	0.0017	*
$x_1\,x_4$	18.15	1	18.15	28.54	0.0001	*
$x_2\,x_3$	25.3	1	25.3	39.79	< 0.0001	**
$x_2\,x_4$	35.05	1	35.05	55.11	< 0.0001	**
$x_3\,x_4$	58.14	1	58.14	91.43	< 0.0001	**
Residual	8.9	14	0.64			
Lack of fit	7.97	10	0.8	3.4	0.1249	NS
Pureerror	0.94	4	0.23			
Cor. total	536.68	28				

[a] DF = Degree of freedom.
[b] Definition of symbols: * represents significant($p < 0.05$); ** represents highly significant($p < 0.0001$); NS = non-significant.

Based on results obtained from the 29 experimental set listed in Table 2, the optimal process variables for acetalization of BzH with EG over the CeFeTiO catalyst may be derived as: EG/BzH molar ratio (x_1) = 1.694, reaction time (x_2) = 2.94 h, amount of catalyst (x_3) = 6.92 wt%, and amount of cyclohexane (x_4) = 12.0 ml at a reaction temperature of 110 °C. As a result, a benzaldehyde ethylene glycol acetal (BEGA) yield of 96.95 % was predicted. To further verify these predicted results, three additional experiments were performed in parallel at 110 °C with somewhat simplified values of x_1 = 1.7 mol/mol, x_2 = 2.9 h, x_3 = 6.9 wt%, and x_4 = 12.0 ml which resulted an experimental BEGA yield of 96.8 %, in good agreement with the optimal experimental value (93.6 %) listed in Table 3.

3.5. Kinetic study

In order to establish the kinetic model for the CeFeTiO catalyst during acetalization of BzH with EG, additional experiments were carried out under reaction conditions optimized by RSM, namely EG/BzH = 1.7 mol/mol, catalyst amount = 6.9 wt%, and amount of cyclohexane = 12 ml under different temperatures (90, 100, 110, and 120 °C) and varied reaction times. During the reaction, *ca.* 1 ml sample was withdrawn from the mixture for analysis at reaction time of 40, 60, 80, 100, and 120 min, respectively. The linear fittings of ln (C_A/C_B) vs. the reaction time at different temperatures based on Eq. (5) were displayed in Fig. 8a. The results clearly indicated that the acetalization reaction of BzH with EG was indeed second-order. The reaction rate constant (k) at different temperatures were further analyzed by the Arrhenius equation

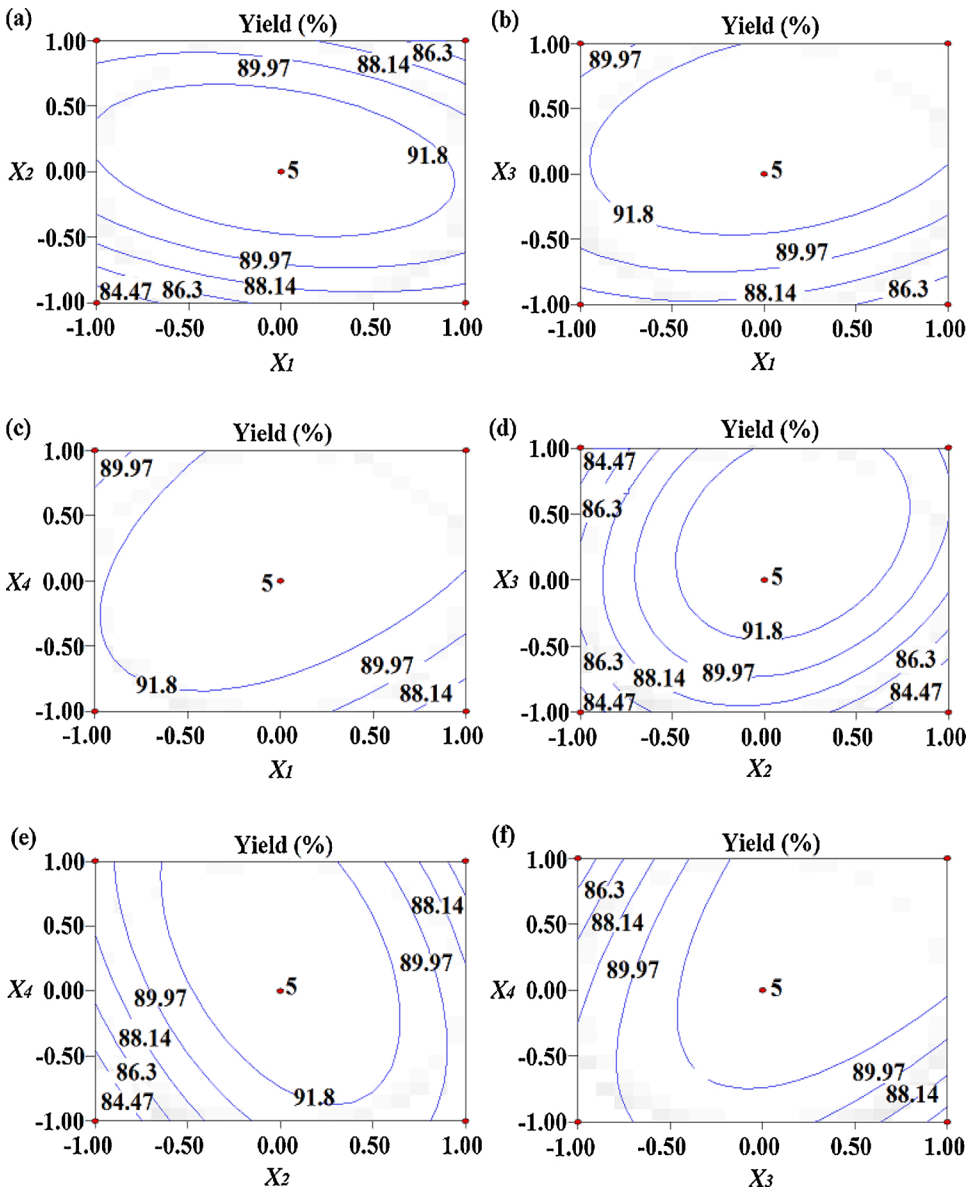

Fig. 6. Contour plots showing variations of a pair of experimental variables (see Table 1) on predicted acetal yields while keeping the other variables at a constant level of 0: (a) $x_1$vsx_2, (b) x_1 vsx_3, (c) x_1 vsx_4, (d) $x_2$vsx_3, (e) x_2 vsx_4, and (f) x_3 vsx_4.

(Eq. (6)) in Fig. 8b. Accordingly, an activation energy (E_a) and a pre-exponential factor (k_0) of 46.65 kJ/mol and 9.7×10^3 L/mol■s, respectively, were deduced. The *Ea* value of the CeFeTiO catalyst in acetalization of BzH with EG was smaller than that of the Amberlyst-15 catalyst in acetalization of ethylaldehyde with glycerol (51.7 kJ/mol) [39] and that of the Amberlyst-47 acidic ion exchange resin in acetalization of *n*-butyraldehydewith glycerol (55.6 kJ/mol) [35]. The above results revealed that CeFeTiO could be considered as a highly effective catalyst for acetalization of benzaldehyde with ethylene glycol.

3.6. Catalyst stability and reusability

The durability and reusability of the CeFeTiO catalyst during the acetalization reaction were further investigated. The test experiments were conducted under the optimized reaction variable obtained from RSM, namely, EG/BzH = 1.7 mol/mol, reaction time = 2.9 h, catalyst amount = 6.9 wt%, amount of cyclohexane = 12 mL, and reaction temperature 110 °C. After each reaction cycle, the spent CeFeTiO catalyst was separated from the reaction system by a simple filtration method, then, washed thoroughly with ethyl acetate to remove organic residues. Finally, the catalyst was dried under vacuum at 70 °C for 10 h without further activation before reuse. As shown in Fig. 9, the CeFeTiO catalyst was highly durable with minor loss in catalytic activity after six consecutive experimental cycles. The BEGA yield decreased marginally from 96.8 % in the first cycle to 90.7 % in the 6th cycle. The gradual decrease in catalytic activity during consecutive cyclic runs was attributed to BET surface area lowering, verified by 94.4 cm^3/g of the fresh catalyst to 81.1 cm^3/g of the spent catalyst after six consecutive runs. It was speculated that gradual diminishing of active sites during recovery and regeneration process may also be accountable for the gradual loss in catalytic activity. In spite of these drawbacks, the aforementioned results indicated that CeFeTiO was indeed a robust catalyst with desirable durability and recyclability for acetalization reactions.

4. Conclusions

In summary, a series of composite metal oxide catalysts were synthesized and applied for acetalization of BzH with EG. The introduction

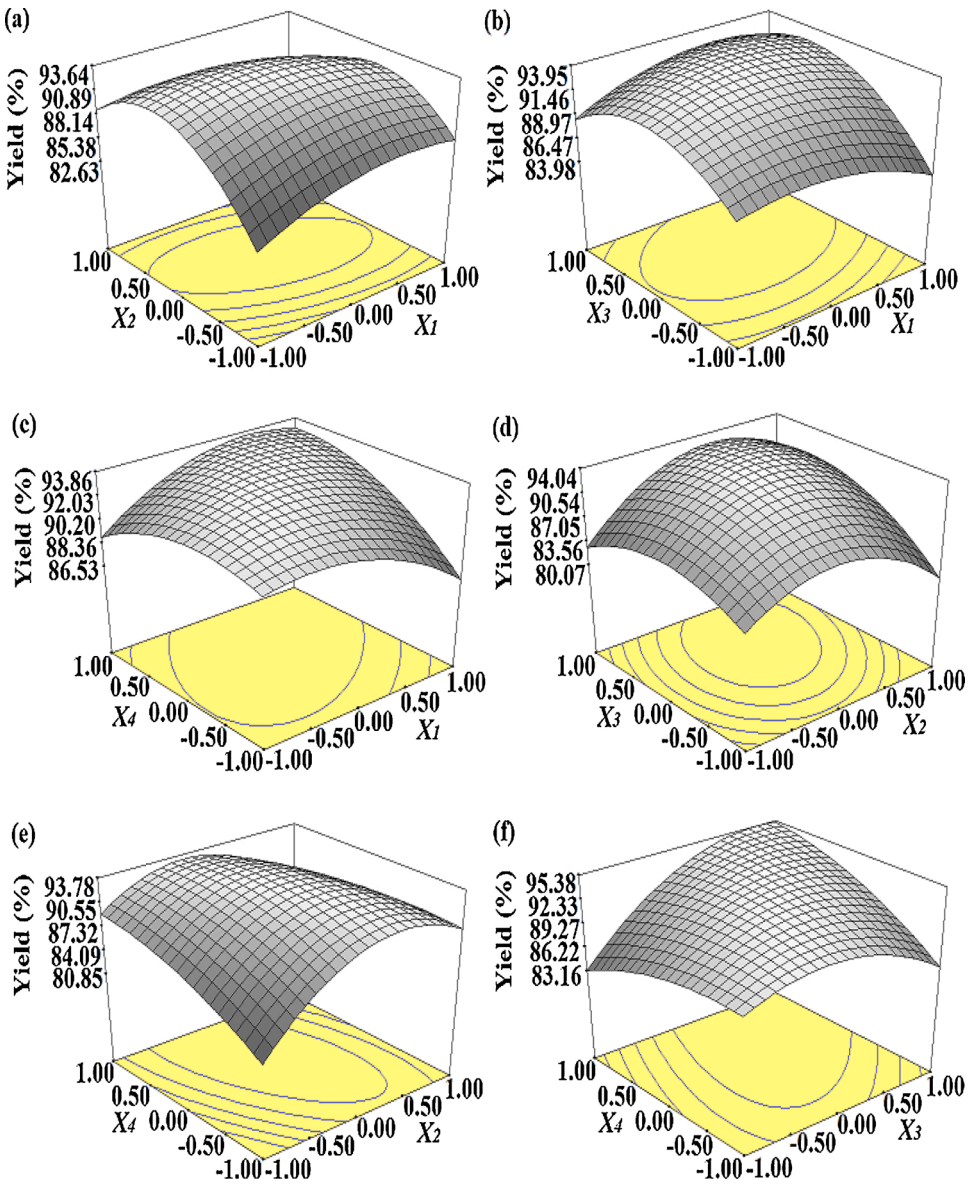

Fig. 7. 3D response surface plots showing variations of a pair of experimental variables (see Table 1) on predicted acetal yields while keeping the other variables at a constant level of 0: (a) $x_1$vs x_2, (b) x_1 vs x_3, (c) x_1 vs x_4, (d) $x_2$vs x_3, (e) x_2 vs x_4, and (f) x_3 vs x_4.

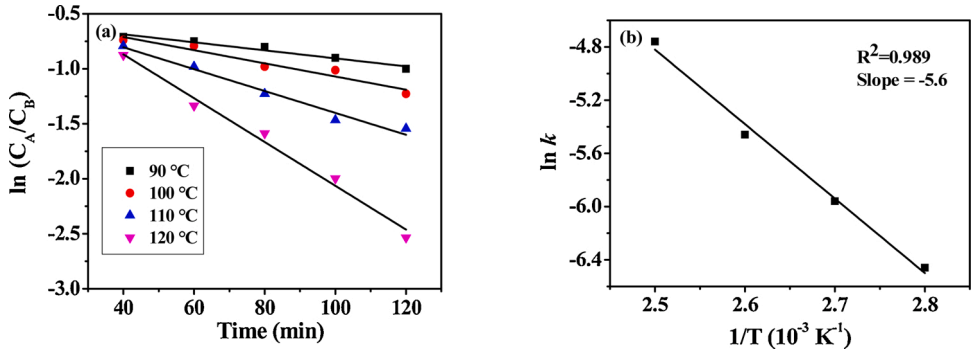

Fig. 8. (a) Variations of ln(C_A/C_B) vs time and (b) Arrhenius plot for acetalization of benzaldehyde with ethylene glycol over the CeFeTiO catalyst. Reation conditions: EG/BzH = 1.7 mol/mol, catalyst amount = 6.9 wt%, and amount of cyclohexane = 12 ml under varied reaction time (40–120 min) and temperatures (90–120 °C).

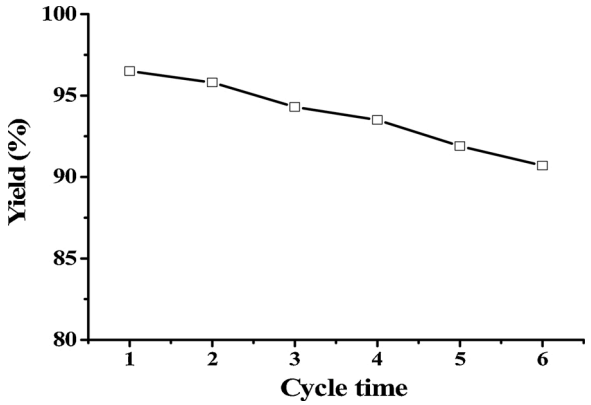

Fig. 9. Stability of the CeFeTiO catalyst during acetalization of benzaldehyde with ethylene glycol. Reaction conditions: EG/BzH = 1.7 mol/mol, reaction time = 2.9 h, catalyst amount = 6.9 wt%, amount of cyclohexane = 12 mL, and reaction temperature 110 °C.

of a third metal promoter onto the pristine bimetallic oxides catalysts, such as FeTiO and CeTiO, notable increased the resultant products' specific surface area, pore volume, as well as acidity. These improved textural and acidic properties induced the catalytic activity enhancement of the corresponding product in acetalization reaction. Among various catalysts examined in this study, the trimetallic CeFeTiO catalyst exhibited superior catalytic activity and acetal yield. The acetalization process taken part in by the CeFeTiO catalyst was optimized by means of response surface methodology (RSM) based on a Box-Behnken design (BBD) with the result of EG/BzH = 1.7 mol/mol, amount of catalyst = 6.9 wt%, reaction time = 2.9 h, and amount of cyclohexane = 12 ml at a reaction temperature of 110 °C. The corresponding acetal yield was 96.8 %, which was in excellent agreement with that predicted by the mathematical model (96.95 %) and the experimental result (93.6 %). In addition, the CeFeTiO composite metal oxide was a robust catalyst with desirable stability and reusability, hence, had potential applications as a solid acidic catalyst in industry, especially in the large-scale acetal manufactures.

CRediT authorship contribution statement

Xiaoxiang Han: Methodology, Investigation, Writing - original draft, Writing - review & editing. **Jinwang Cai:** Investigation, Data curation, Writing - review & editing. **Xiaorui Mao:** Validation, Data curation, Writing - review & editing. **Xinya Yang:** Resources, Data curation. **Linyan Qiu:** Resources, Data curation. **Fanghao Li:** Resources, Data curation. **Xiujuan Tang:** Resources, Data curation. **Yanbo Wang:** Writing - review & editing. **Shang-Bin Liu:** Writing - review & editing.

Declaration of Competing Interest

The authors report no declarations of interest.

References

[1] D.M. Clode, Chem. Rev. 79 (1979) 555–563, https://doi.org/10.1021/cr60322a002.
[2] G. Sartori, R. Ballini, F. Bigi, G. Bosica, R. Maggi, P. Righi, Chem. Rev. 35 (2010) 199–250, https://doi.org/10.1021/cr0200769.
[3] R.J. Linderman, S. Chen, Tetrahedron Lett. 37 (1996) 3819–3822, https://doi.org/10.1016/0040-4039(96)00722-8.
[4] M.J. Climent, A. Velty, A. Corma, Green Chem. 4 (2002) 565–569, https://doi.org/10.1039/b207506g.
[5] L. Chen, B. Nohair, S. Kaliaguine, Appl. Catal. A-Gen. 509 (2016) 143–152, https://doi.org/10.1016/j.apcata.2015.08.014.
[6] C. Ferreira, A. Araujo, V. Calvino-Casilda, M.G. Cutrufello, E. Rombi, A.M. Fonseca, M.A. Banares, I.C. Neves, Microporous Mesoporous Mater. 271 (2018) 243–251, https://doi.org/10.1016/j.micromeso.2018.06.010.
[7] J. Zhou, Z. Dong, H. Yang, Z. Shi, X. Zhou, R. Li, Appl. Surf. Sci. 279 (2013) 360–366, https://doi.org/10.1016/j.apsusc.2013.04.113.
[8] J.M. Rubiocaballero, S. Saravanamurugan, P. Mairelestorres, A. Riisager, Catal. Today 234 (2014) 233–236, https://doi.org/10.1016/j.cattod.2014.03.004.
[9] X. Hong, O. Mcgiveron, A.K. Kolah, A. Orjuela, L. Peereboom, C.T. Lira, D.J. Miller, Chem. Eng. J. 222 (2013) 374–381, https://doi.org/10.1016/j.cej.2013.02.023.
[10] F. Frusteri, L. Spadaro, C. Beatrice, C. Guido, Chem. Eng. J. 134 (2007) 239–245, https://doi.org/10.1016/j.cej.2007.03.042.
[11] L. Fang, K. Zhang, L. Chen, P. Wu, Chin. J. Catal. 34 (2013) 932–941, https://doi.org/10.1016/s1872-2067(12)60591-9.
[12] X. Han, W. Yan, K. Chen, C. Hung, L. Liu, P. Wu, S. Huang, S. Liu, Appl. Catal. A-Gen 485 (2014) 149–156, https://doi.org/10.1016/j.apcata.2014.08.001.
[13] J. Miao, H. Wan, Y. Shao, G. Guan, B. Xu, J. Mol. Catal. A-Chem. 348 (2011) 77–82, https://doi.org/10.1016/j.molcata.2011.08.005.
[14] S.S. Poly, M.A.R. Jamil, A.S. Touchy, S. Yasumura, S.H. Hakim, T. Toyao, Z. Maeno, K. Shimizu, Mol. Catal. 479 (2019) 110608–110613, https://doi.org/10.1016/j.mcat.2019.110608.
[15] B.R. Jermy, A. Pandurangan, Appl. Catal. A-Gen. 295 (2005) 185–192, https://doi.org/10.1016/j.apcata.2005.08.018.
[16] B. Mallesham, P. Sudarsanam, G. Raju, B.M. Reddy, Green Chem. 15 (2013) 478–489, https://doi.org/10.1039/c2gc36152c.
[17] J. Deutsch, A. Martin, H. Lieske, J. Catal. 245 (2007) 428–435, https://doi.org/10.1016/j.jcat.2006.11.006.
[18] P. Manjunathan, S.P. Maradur, A.B. Halgeri, G.V. Shanbhag, J. Mol. Catal. A-Chem. 396 (2015) 47–54, https://doi.org/10.1016/j.molcata.2014.09.028.
[19] L. Li, T.I. Korányi, B.F. Sels, P.P. Pescarmona, Green Chem. 14 (2012) 1611–1619, https://doi.org/10.1039/c2gc16619d.
[20] F. Zhang, J. Shi, Y. Jin, Y. Fu, Y. Zhong, W. Zhu, Chem. Eng. J. 259 (2015) 183–190, https://doi.org/10.1016/j.cej.2014.07.119.
[21] B. Thomas, V.G. Ramu, S. Gopinath, J. George, M. Kurian, G. Laurent, G.L. Drisko, S. Sugunan, Appl. Clay Sci. 53 (2011) 227–235, https://doi.org/10.1016/j.clay.2011.01.021.
[22] T. Kawabata, T. Mizugaki, K. Ebitani, K. Kaneda, Tetrahedron Lett. 42 (2001) 8329–8332, https://doi.org/10.1016/s0040-4039(01)01788-9.
[23] J. Tateiwa, H. Horiuchi, S. Uemura, Cheminform 60 (1995) 4039–4043, https://doi.org/10.1021/jo00118a021.
[24] T.F. Parangi, B.N. Wani, U.V. Chudasama, Ind. Eng. Chem. Res. 52 (2013) 8969–8977, https://doi.org/10.1021/ie400686d.
[25] A. Dhakshinamoorthy, M. Alvaro, H. Garcia, Adv. Synth. Catal. 352 (2010) 3022–3030, https://doi.org/10.1002/adsc.201000537.
[26] R. Rodrigues, D. Mandelli, N.S. Gonçalves, P.P. Pescarmona, W.A. Carvalho, J. Mol. Catal. A-Chem. 422 (2016) 122–130, https://doi.org/10.1016/j.molcata.2016.02.002.
[27] M.A. Olutoye, S.C. Lee, B.H. Hameed, Bioresour. Technol. 102 (2011) 10777–10783, https://doi.org/10.1016/j.biortech.2011.09.033.
[28] M.A. Olutoye, B.H. Hameed, Fuel Process. Technol. 91 (2010) 653–659, https://doi.org/10.1016/j.fuproc.2010.01.014.
[29] N.R.E. Radwan, Appl. Catal. A-Gen. 299 (2006) 103–121, https://doi.org/10.1016/j.apcata.2005.10.008.
[30] M.A. Olutoye, C.P. Wong, L.H. Chin, B.H. Hameed, Fuel Process. Technol. 124 (2014) 54–60, https://doi.org/10.1016/j.fuproc.2014.02.013.
[31] J.A. Melero, L.F. Bautista, G. Morales, J. Iglesias, R. Sánchez-Vázquez, Chem. Eng. J. 161 (2010) 323–331, https://doi.org/10.1016/j.cej.2009.12.037.
[32] V. Vishwanathan, K.W. Jun, J.W. Kim, H.S. Roh, Appl. Catal. A-Gen. 276 (2004) 251–255, https://doi.org/10.1016/j.apcata.2004.08.011.
[33] R. Jin, Y. Liu, Z. Wu, H. Wang, T. Gu, Catal. Today 153 (2010) 84–89, https://doi.org/10.1016/j.cattod.2010.01.039.
[34] C. Fang, D. Zhang, L. Shi, R. Gao, H. Li, L. Ye, J. Zhang, Catal. Sci. Technol. 3 (2013) 803–811, https://doi.org/10.1039/c2cy20670f.
[35] M.B. Güemez, J. Requies, I. Agirre, P.L. Arias, V.L. Barrio, J.F. Cambra, Chem. Eng. J. 228 (2013) 300–307, https://doi.org/10.1016/j.cej.2013.04.107.
[36] W. Peng, J. Feng, Y. Zhao, S. Wang, J. Liu, ACS Appl. Mater. Interfaces 8 (2016), https://doi.org/10.1021/acsami.6b08057, 33755-23762.
[37] W. Peng, Y. Zhao, J. Liu, Sci. Bull. 63 (2018) 252–266, https://doi.org/10.1016/j.scib.2018.01.017.
[38] X. Han, K. Ouyang, C. Xiong, X. Tang, Q. Chen, K. Wang, L. Liu, C. Hung, S. Liu, Appl. Catal. A-Gen. 543 (2017) 115–124, https://doi.org/10.1016/j.apcata.2017.06. 024.
[39] R.P.V. Faria, C.S.M. Pereira, V.M.T.M. Silva, J.M. Loureiro, A.E. Rodrigues, Ind. Eng. Chem. Res. 52 (2013) 1538–1547, https://doi.org/10.1021/ie302935w.